Induction Motor Parameter Tuning for High-Performance Drives

Jul-Ki Seok, *Member, IEEE,* and Seung-Ki Sul, *Fellow, IEEE*

***Abstract*—A new approach to parameter tuning of induction motors in the course of drive commissioning is proposed. Usually, the motors originate from different manufacturers, and so the parameters are not known prior to startup of the drive. The control system of the drive utilizes the parameters obtained by extraneous tests and based on a number of assumptions that are not valid under all operating conditions. Therefore, completion of the tuning of all motors at an industrial site is quite time consuming, and it is a very difficult job, even to skilled engineers. To overcome these problems, the proposed tuning procedure is sensitive to detuning and independent of information on other parameters. The state of detuning is clearly noticeable in the shape of the controller output signal of the drive system. The proposed scheme has the advantage of being general and readily applicable to a wide range of other systems, such as ac/dc boost converters, surface-mounted permanent-magnet synchronous motors, interior permanent-magnet synchronous motors, and so on. Experimental results are offered to validate the feasibility of the proposed tuning algorithm.**

***Index Terms*—Controller output signal, drive commissioning, induction motor, parameter tuning.**

I. Introduction

THE demand for high-performance induction motor drives has been experiencing a steady rise in the industry and the sophistication in the control techniques employed has been escalating in direct proportion. One such control strategy, which has generated widespread interest, is the vector control technique that provides a method for decoupling the torque- and flux-producing currents in an induction motor [1]. However, precise decoupling control of an induction motor requires accurate motor parameters which must be measured or estimated [2]. When incorrect parameter values are used in the controller, it may cause instantaneous errors in both torque and flux, resulting in sluggish dynamics. In the modern steel mill plant, for example, there are some main motors and a tremendous number of auxiliary motors to be tuned. In many cases, the motors in the plant originate from different manufacturers, and so the parameters are not known prior to startup of the drive. Moreover, in some online parameter adaptation algorithms, if initial an parameter value of the unknown motor is apart from the actual one, their rate of convergence is often disappointing.

Paper IPCSD 00–045, presented at the 1998 Industry Applications Society Annual Meeting, St. Louis, MO, October 12–16, and approved for publication in the IEEE TRANSACTIONS ON INDUSTRY APPLICATIONS by the Industrial Drives Committee of the IEEE Industry Applications Society. Manuscript submitted for review May 7, 1999 and released for publication October 20, 2000.

J.-K. Seok is with the Production Engineering Center, Samsung Electronics Company Ltd., Suwon City 442-742, Korea (e-mail: doljk@samsung.com).

S.-K. Sul is with the School of Electrical Engineering, Seoul National University, Seoul 151-742, Korea (e-mail: sulsk@plaza.snu.ac.kr).

Publisher Item Identifier S 0093-9994(01)00908-2.

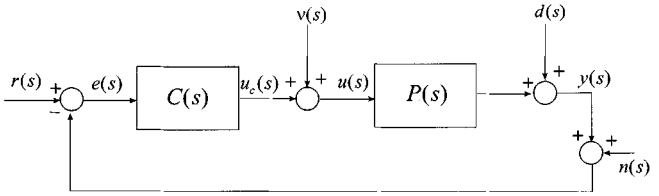

Fig. 1. Classical control loop including model uncertainty, disturbance, and noise.

To overcome these problems, a great deal of research has been conducted concerning the determination of the unknown induction motor prior to starting [3]–[6]. However, these conventional techniques for determining motor parameters sometimes have the drawback that they are based on a number of assumptions that are not valid under all operating conditions. More recently, the time-domain and frequency-domain tests have been proposed [7]–[11]. They might be expensive to perform, require special test equipment, and have a low sensitivity to detuning. In addition, some of them simplify the problem by assuming that all the other parameters are exactly known, except the parameter under consideration. Therefore, completion of the tuning of all motors in the plant is quite time consuming, and it is a very difficult job to commissioning engineers. Observing multiple data of parameters during the tuning procedure simultaneously, skilled engineers are often required to make tough decisions based on their experience and empirical knowledge. In order to reduce the cost of commissioning and to make control performance prior to startup more reliable, the initial parameter tuning of an induction motor should be sensitive to detuning and independent of information of other parameters.

In this paper, a new technique for identifying the state of tuning of a vector controller prior to actual starting of unknown motor is presented. The proposed method successfully determines all electrical parameters in an induction motor except stator resistance by monitoring the speed and/or current controller output signal of the drive. The state of detuning is clearly noticeable in the shape of the controller output signal, which has a high sensitivity to detuning. In this approach, each tuning procedure is inherently independent of the information of other parameters.

II. Principle of Parameter Tuning Algorithm

In this section, some classical control ideas are reviewed to introduce the principle of the parameter tuning algorithm. In

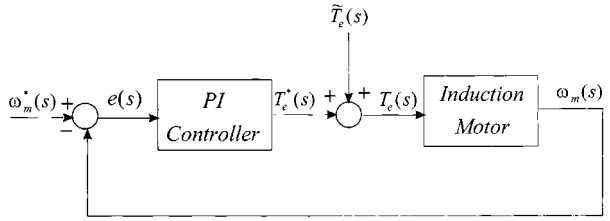

Fig. 2. Block diagram of closed-loop speed control system.

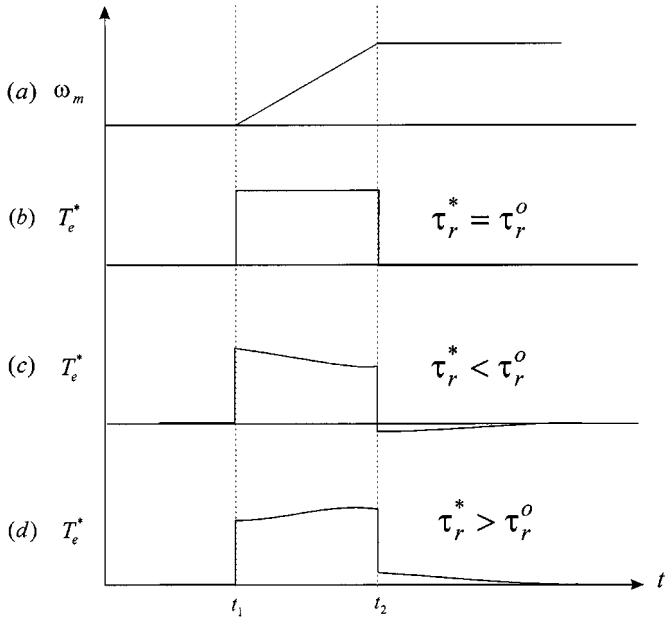

Fig. 3. Controller output response for rotor time constant tuning or detuning.

Fig. 1, the quantities r, e, and u are the reference input, the measured tracking error, and the plant input, respectively. The quantitiesy u_c, y, and v represent the controller output, the plant output, and the plant uncertainty, respectively, and d and n indicate the system disturbance and measurement noise. $P(s)$ and $C(s)$ represent the transfer function of the plant and that of the controller, respectively.

Then, the following equations are easily established:

$$y(s) = \frac{C(s)P(s)}{1+C(s)P(s)}(r(s)-n(s)) + \frac{P(s)}{1+C(s)P(s)}\nu(s) + \frac{1}{1+C(s)P(s)}d(s). \quad (1)$$

$$u_c(s) = \frac{C(s)}{1+C(s)P(s)}(r(s)-d(s)) + \frac{C(s)P(s)}{1+C(s)P(s)}C(s)\cdot n(s) - \frac{C(s)P(s)}{1+C(s)P(s)}\nu(s). \quad (2)$$

Generally, for good tracking, $C(s)$ would be selected so that $|C(s)P(s)| \gg 1$ [12]. In this system, it can be assumed that there is no system disturbance and it is possible to use sensors with acceptably low noise in the frequency ranges to be controlled, that is, in the frequencies where y is to track r. This is a reasonably accurate assumption for many drives with

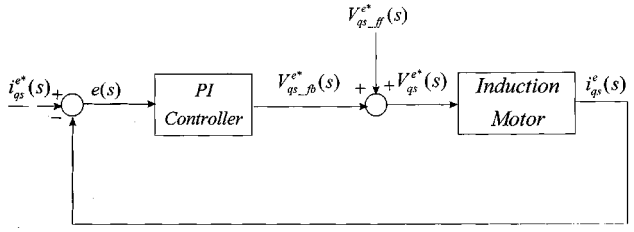

Fig. 4. Block diagram of synchronous q-axis current control system.

TABLE I
RATINGS AND PARAMETERS OF INDUCTION MACHINE UNDER TEST

Rated power output[kW]	22
Rated voltage[V]	220
Number of poles	4
Stator resistance[Ω]	0.238
Rotor resistance[Ω]	43.0
Mutual inductance[mH]	3.5
Stator transient inductance[mH]	1.1
Moment of inertia[Kg-m^2]	0.16

vector control prior to startup. Under this assumption, (2) can be rewritten as

$$u_c(s) = \frac{C(s)}{1+C(s)P(s)}r(s) - \frac{C(s)P(s)}{1+C(s)P(s)}\nu(s) \cong \frac{C(s)}{1+C(s)P(s)}r(s) - \nu(s). \quad (3)$$

In (3), the effect of the plant uncertainty directly appears on the controller output signal. Therefore, observing the controller output signal which reflects the model uncertainty, the state of parameters detuning is clearly noticeable. In this approach, the tuning procedure is inherently independent of information of other parameters.

III. Parameter Tuning Procedure

A. Rotor Time Constant Tuning

Industry standard speed control topology with an induction motor is shown in Fig. 2. Here, the plant under consideration may be an induction motor drive system using the indirect vector control method, and the proportional plus integral (PI) controller is used to generate the torque reference $T_e^*(s)$ in response to the speed error. When the rotor time constant is incorrect in the indirect vector controller, the calculated slip frequency is incorrect and the flux angle is no longer appropriate for field orientation [1]. As a result, the distorted torque $\tilde{T}_e(s)$ due to rotor time constant mismatch is generated and directly added to the controller output $T_e^*(s)$ as (3), while the speed response $\omega_m(s)$ tracks with the reference speed $\omega_m^*(s)$.

When the speed reference profile shown in Fig. 3(a) is used to prevent saturation of the speed controller, the speed controller output behaviors according to the state of tuning and detuning can be predicted. The detuned cases in Fig. 3(c) and (d) produce a distorted response unlike the tuned case in Fig. 3(b). Thus,

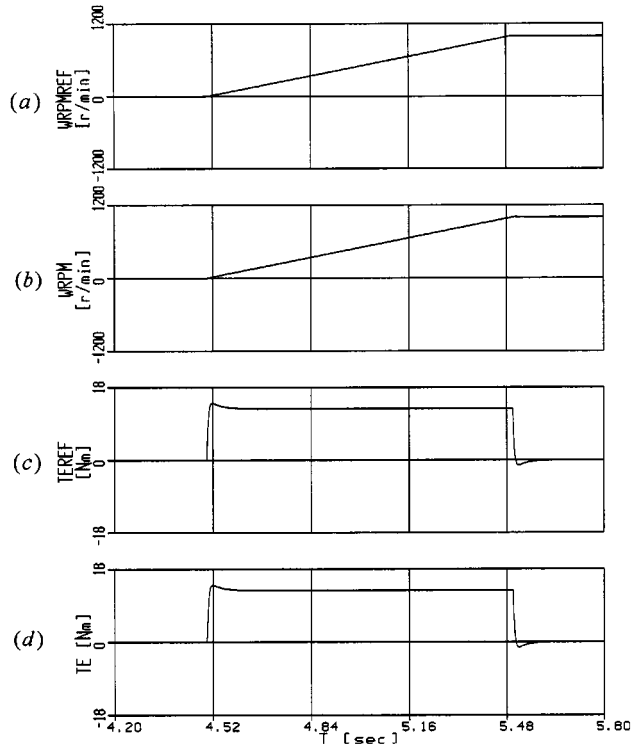

Fig. 5. Speed controller output without rotor time constant error and noise. (a) Speed reference trajectory. (b) Speed feedback. (c) Torque reference. (d) Actual torque.

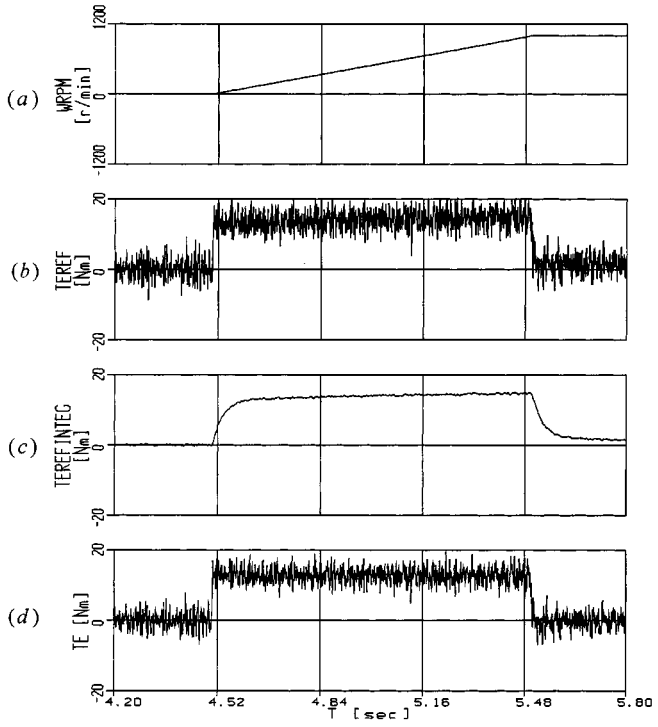

Fig. 6. Speed controller output with detuned rotor time constant ($\tau_r^* = 1.2 \cdot \tau_r^o$). (a) Speed feedback. (b) Torque reference. (c) Integral term of speed controller. (d) Actual torque.

if the speed controller output signal is considered as a tuning performance index for the rotor time constant, the state of tuning or detuning is clearly noticeable.

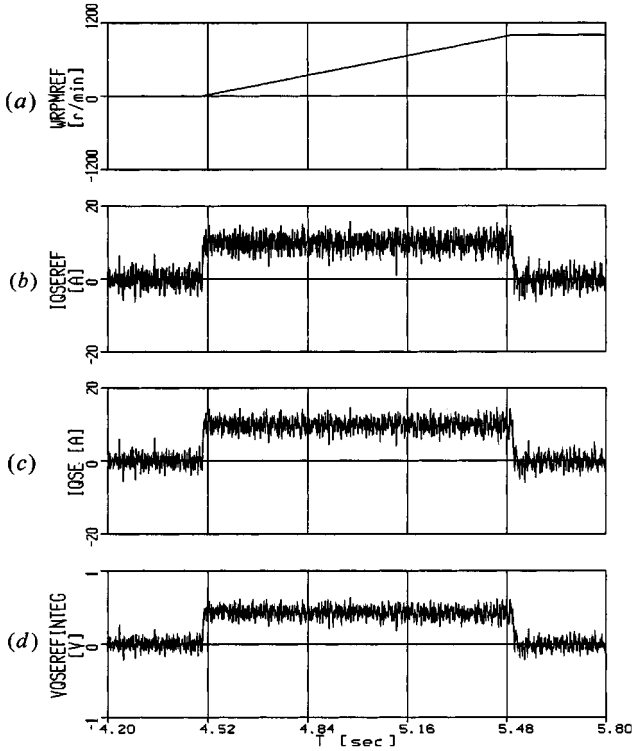

Fig. 7. Current controller output with tuned stator inductance ($L_s^* = L_s^o$). (a) Speed reference trajectory. (b) q-axis current reference. (c) q-axis current. (d) Integral term of q-axis current controller.

B. Inductance Tuning

Current control in the synchronous reference frame is often accomplished through the compensation of the induction motor back-EMF voltage component by the feedforward manner as shown in Fig. 4 [13]. In Fig. 4, $V_{qs\_fb}^{e*}(s)$ is the dynamic voltage which decides the transition of the q-axis current, $V_{qs\_ff}^{e*}(s)$ is the q-axis motor back-EMF voltage, and $V_{qs}^{e*}(s)$ is the reference voltage. In steady state, q-axis motor back EMF can be obtained as

$$V_{qs\_ff}^{e*} = \omega_e L_s^o i_{ds}^e - \omega_{sl} \frac{L_m^{o2}}{L_r^o} i_{ds}^e. \tag{4}$$

In the above equation, ω_e is the synchronous angular velocity, L_s^o is the actual stator inductance in the motor, and ω_{sl} is the slip angular velocity. i_{ds}^e indicates the d-axis current in the synchronously rotating reference frame, and L_m^o and L_r^o represent the actual magnetizing and rotor inductance in the motor, respectively. In (4), except for the low-speed operation region, the second term on the right-side hand is so small compared to the first term that it could be neglected in practice. For example, the induction motor used in our experiment, whose parameters are shown in Table I, has $\omega_e L_s^o i_{ds}^e \cong 56$ V and $\omega_{sl}(L_m^{o2}/L_r^o) i_{ds}^e \cong 0.4$ V when the motor speed changes at 600 r/min which is about one-third of rated speed. Thus, the first term $\omega_e L_s^o i_{ds}^e$ is larger than the second term $\omega_{sl}(L_m^{o2}/L_r^o) i_{ds}^e$ by $10\times$.

Neglecting $\omega_{sl}(L_m^{o2}/L_r^o) i_{ds}^e$ in (4), the motor back EMF can be given by

$$V_{qs\_ff}^{e*} \cong \omega_e L_s^o i_{ds}^e = \omega_e L_s^* i_{ds}^e + \omega_e \Delta L_s i_{ds}^e \tag{5}$$

where L_s^* is the stator inductance in the controller and ΔL_s indicates the error between L_s^o and L_s^*. If an error due to stator inductance detuning exists, $\omega_e \Delta L_s i_{ds}^e$ is directly added to the controller output $V_{qs\_fb}^{e*}(s)$ as (3), while the q-axis current $i_{qs}^e(s)$ tracks the reference current $i_{qs}^{e*}(s)$. Thus, observing the q-axis current controller output signal, the stator inductance in an induction motor can be tuned.

Generally, it should be noted that the magnetizing curve of an induction motor can be obtained from a no-load or open-loop V/Hz test. However, the no-load test requires test equipment such as an adjustable voltage regulator [3]. Moreover, the open-loop V/Hz test at low frequency suffers the stability problem that becomes even worse for high-power drives, high-efficiency-motors, and high-switching-frequency operation [14]. Using the proposed tuning method, the values of magnetizing inductance over a range of i_{ds}^e are simply obtained at all operating conditions, maintaining i_{ds}^e at the desired value.

Also, (4) can be rewritten as

$$\begin{aligned} V_{qs\_ff}^{e*} &= \omega_e L_\sigma^o i_{ds}^e + \omega_r \frac{L_m^o}{L_r^o} \lambda_{dr}^e - \frac{L_m^o}{\tau_r^o L_r^o} \lambda_{qr}^e \\ &\cong \omega_e L_\sigma^* i_{ds}^e + \omega_e \Delta L_\sigma i_{ds}^e + \omega_r \frac{L_m^o}{L_r^o} \lambda_{dr}^{e*} \end{aligned} \tag{6}$$

where L_σ^* is the stator transient inductance in the controller and ΔL_σ indicates the error between L_σ^o and L_σ^*.

In (6), λ_{dr}^e and λ_{qr}^e indicate the d–q–axes rotor flux in the synchronously rotating reference frame, ω_r is the rotor angular velocity, and τ_r^o represents the actual rotor time constant in the motor. Since the stator inductance has been previously tuned, the producing flux λ_{dr}^e in (6) is almost same as the rotor flux λ_{dr}^{e*} in the controller. Therefore, the error of back-EMF voltage is mainly due to the detuning of stator transient inductance and this error voltage which is proportional to the motor speed directly appears in the controller output $V_{qs\_fb}^{e*}(s)$. With the feedforward voltage inadequately compensating for the detuning in motor inductance, the controller output voltage becomes distorted according to the change of motor speed.

IV. Simulation Results

Several simulations have been carried out to examine the feasibility of the proposed tuning algorithm. Table I shows the rated values and the nominal parameters of a tested machine. The switching device is assumed to be an insulated gate bipolar transistor (IGBT) of 3-kHz switching frequency and the sampling periods of current and speed control loop are 167 μs and 1 ms, respectively. The cutoff frequencies of the current controller and speed controller is selected to 2000 and 200 rad/s.

Fig. 5 shows the simulation waveforms under the condition where the speed is brought up to 1000 r/min with no load torque on the motor. These plots correspond to the ideal case without parameter uncertainty and noise. Fig. 5(a) and (b) shows the plot of speed reference and feedback and Fig. 5(c) and (d) shows the torque reference and actual torque. In the ideal case, as shown in Fig. 5(c) and (d), the actual torque is exactly identical to the reference torque.

Fig. 6 shows the responses of the speed control system to represent possible rotor time constant uncertainty that is considered +20% off from its tuned value. In this test, noisy inputs of the speed and current sensors are given to the drive system. Speed sensor measurement is corrupted with zero-mean Gaussian distributed measurement noise with ±0.028% deviation of rated speed, and the current sensor measurement noise level is set to be ±0.74% mean and ±0.74% deviation of rated current. The level of noise is thought to be higher than would be encountered in most practical situations.

The speed feedback and reference torque are depicted in Fig. 6(a) and (b), respectively. A chatter is produced due to a speed measurement noise as seen in the plot of reference torque and actual torque. Observing the reference torque, it is somewhat difficult to distinguish between the tuned and detuned case. To circumvent this problem, the integral term of the speed controller as shown in Fig. 6(c) is used for the tuning signal. The integral term is less noisy and still shows a good reflection of rotor time constant mismatch despite the measurement noise. Even in a small amount of error, the state of tuning in the detuned case is clearly noticeable compared with that in the tuned case.

Fig. 7 shows the responses of the current control system when the stator inductance is tuned. The simulation traces shown in Fig. 8(a) and (b) are obtained under the detuned condition where the stator inductance is overestimated by 20% of the tuned value. The traces in Fig. 8(c) and (d) are under detuned condition underestimated by 20%. The reference speed changes from 0 to 1000 r/min, as shown in Fig. 7(a). The q-axis current in Figs. 7(c) and 8(b) and (d) tracks the reference current in Fig. 7(b) during acceleration. In the detuned case, the error component in the feedforward voltage is added to the controller output so that the integral term of the q-axis current controller in Fig. 8(a) and (c) is increased or decreased according to the change of motor speed.

The simulation traces shown in Fig. 9(a) and (b) are obtained under detuned condition where the stator transient inductance is overestimated by 20% of tuned value. The traces in Fig. 9(c) and (d) are under detuned condition underestimated by 20%. With the feedforward voltage inadequately compensating for the detuning in the stator transient inductance, the controller output voltage in Fig. 9(a) and (c) provides a useful indicator of the accuracy of stator transient inductance tuning.

V. Experimental Results

Extensive tests are performed to evaluate the feasibility of the presented study. The algorithm is programmed and installed on an actual IGBT inverter to drive a 22-kW induction machine whose parameters are listed in Table I. In all traces included herein, the internal signal is available at the output of the monitoring D/A converter built into the drive.

Figs. 10 and 11 show the responses of the speed control system when the rotor time constant is tuned and overestimated by 20% of tuned value, respectively. The reference speed changes from 500 to 1500 r/min to avoid speed measurement error in the low-speed region as shown in Figs. 10 and 11(a) and the motor is running with no load in Figs. 10 and 11(b). In

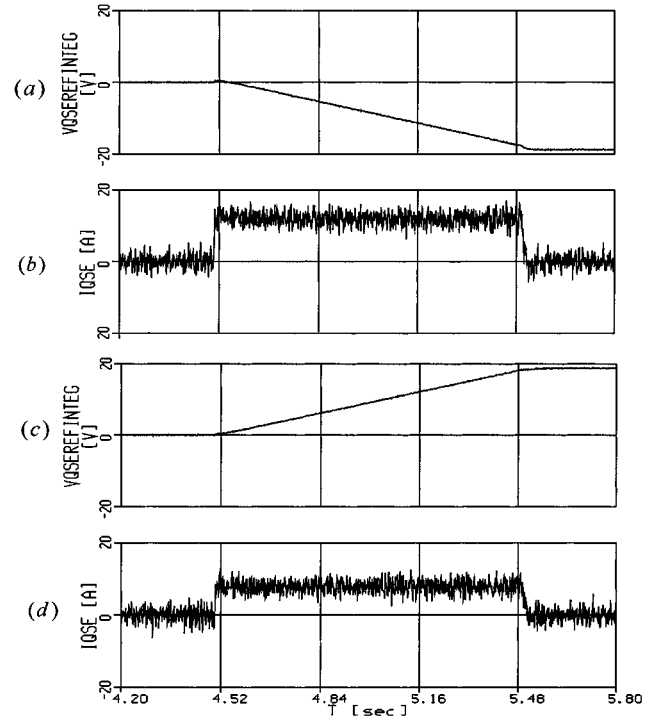

Fig. 8. Current controller output with detuned stator inductance. (a), (b) $L_s^* = 1.2 \cdot L_s^o$. (c), (d) $L_s^* = 0.8 \cdot L_s^o$.

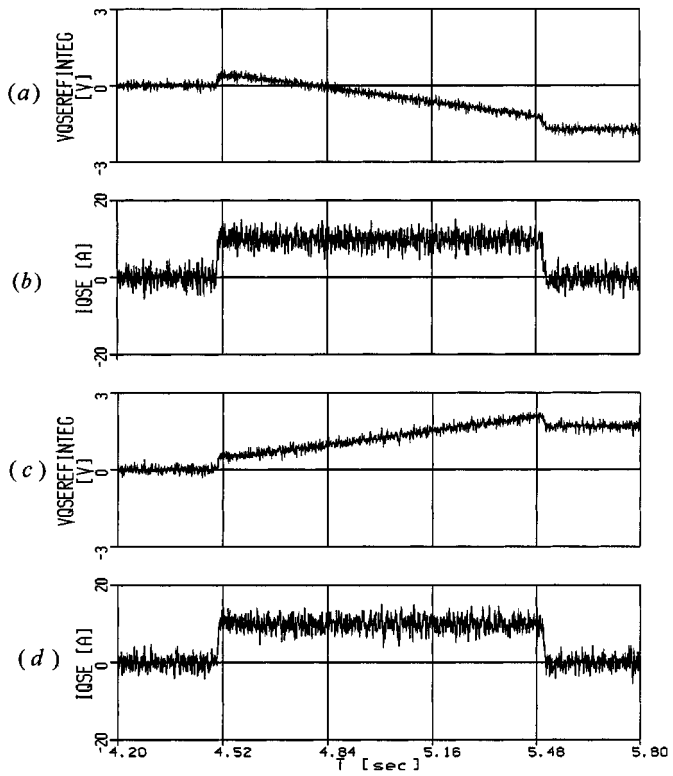

Fig. 9. Current controller output with detuned stator transient inductance. (a), (b) $L_\sigma^* = 1.2 \cdot L_\sigma^o$. (c), (d) $L_\sigma^* = 0.8 \cdot L_\sigma^o$.

Figs. 10 and 11(c), the reference torque is depicted and a chatter is produced due to a speed measurement noise. Observing the reference torque, it is somewhat difficult to distinguish between the tuned and detuned case. To circumvent this problem, the

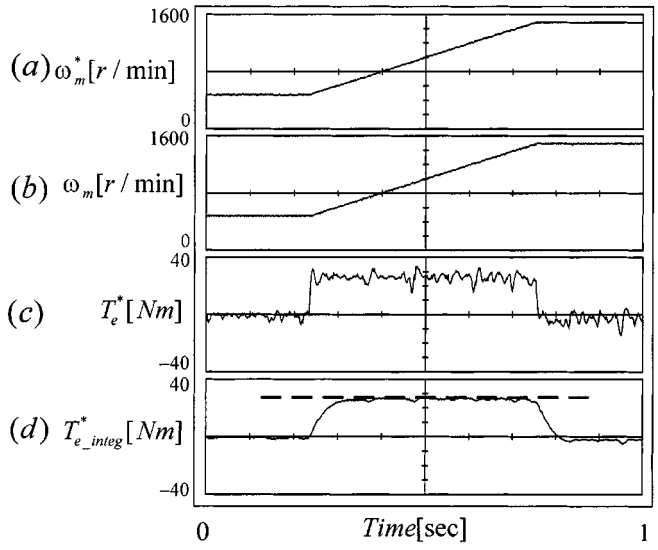

Fig. 10. Speed controller output with tuned rotor time constant ($\tau_r^* = \tau_r^o$). (a) Speed reference trajectory. (b) Speed feedback. (c) Torque reference. (d) Integral term of speed controller.

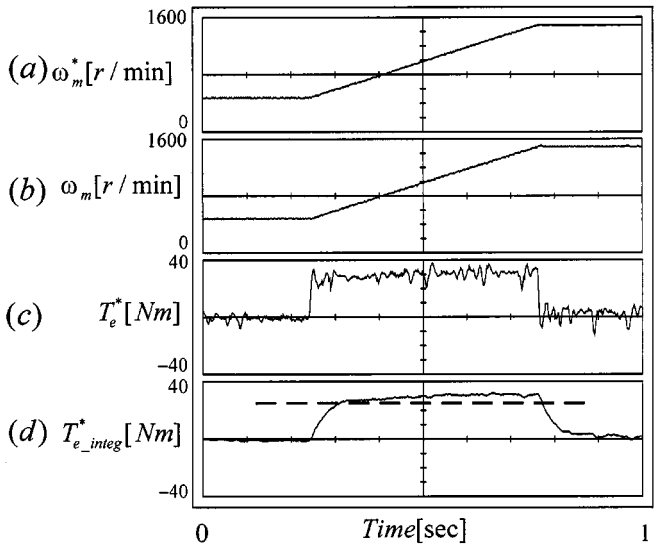

Fig. 11. Speed controller output with detuned rotor time constant ($\tau_r^* = 1.2 \cdot \tau_r^o$). (a) Speed reference trajectory. (b) Speed feedback. (c) Torque reference. (d) Integral term of speed controller.

integral term of the speed controller is shown in Figs. 10 and 11(d). The integral term is less noisy and still provides a useful indicator of the accuracy of rotor time constant tuning, even in the presence of system noise. The experimental results are in good agreement with the simulation results shown in Figs. 5 and 6.

Figs. 12 and 13 show the responses of the current control system when the stator inductance is tuned and is overestimated by 20% of tuned value, respectively. The reference speed changes from 300 to 600 r/min as shown in Figs. 12 and 13(a) and the q-axis current in Figs. 12 and 13(c) tracks the reference current in Figs. 12 and 13(b) during acceleration. In the detuned case, the error component in the feedforward voltage is added to the controller output so that the integral term of the q-axis current controller in Fig. 13(d) is increased or decreased according to the change of motor speed.

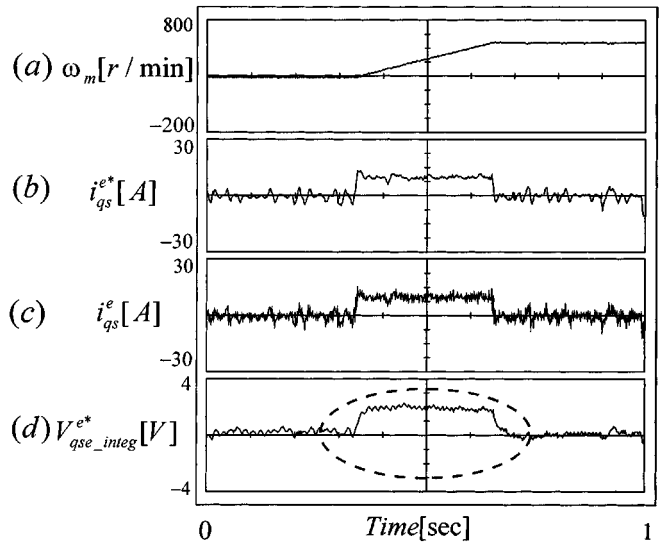

Fig. 12. Current controller output with tuned stator inductance ($L_s^* = L_s^o$). (a) Speed reference trajectory. (b) q-axis current reference. (c) q-axis current. (d) Integral term of q-axis current controller.

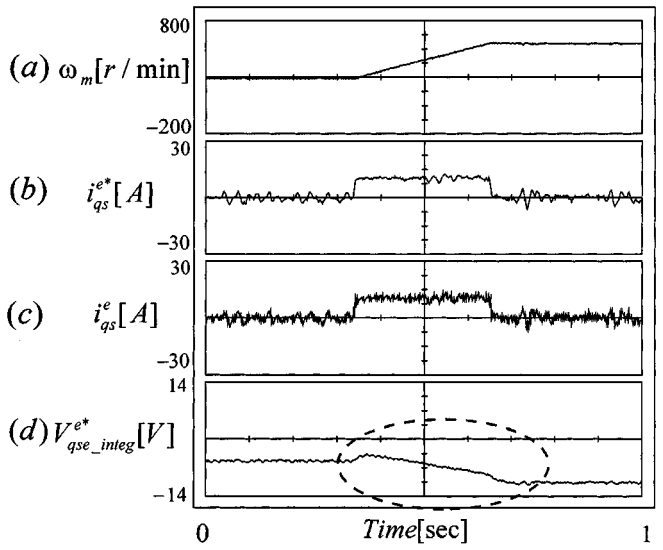

Fig. 13. Current controller output with detuned stator inductance ($L_s^* = 1.2 \cdot L_s^o$). (a) Speed reference trajectory. (b) q-axis current reference. (c) q-axis current. (d) Integral term of q-axis current controller.

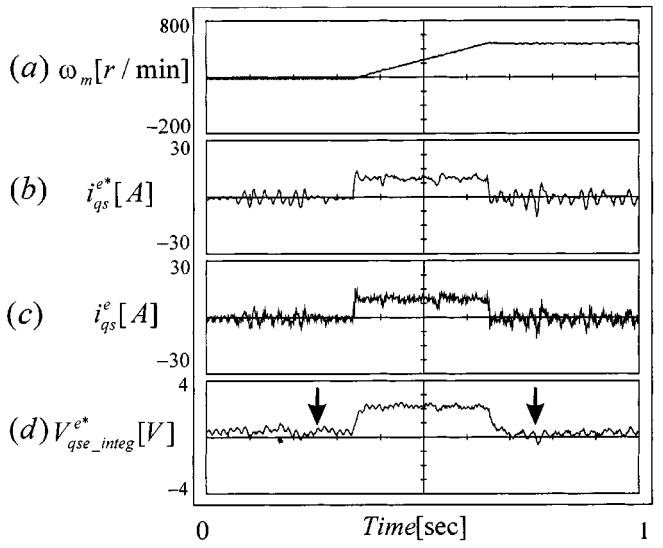

Fig. 14. Current controller output with tuned stator transient inductance ($L_\sigma^* = L_\sigma^o$). (a) Speed reference trajectory. (b) q-axis current reference. (c) q-axis current. (d) Integral term of q-axis current controller.

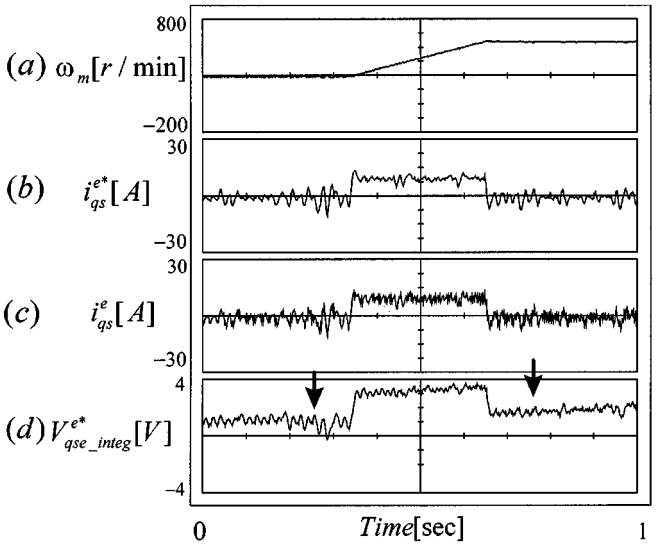

Fig. 15. Current controller output with detuned stator transient inductance ($L_\sigma^* = 0.8 \cdot L_\sigma^o$). (a) Speed reference trajectory. (b) q-axis current reference. (c) q-axis current. (d) Integral term of q-axis current controller.

Figs. 14 and 15 show the responses of the current control system when the stator transient inductance is tuned and is detuned by -20%, respectively. With the feedforward voltage inadequately compensating for the detuning in the stator transient inductance, the controller output voltage in Fig. 15(d) becomes distorted, unlike that in Fig. 14(d). From these results, it is verified that the proposed method is sensitive even to a small error in the motor parameters and does not require the information of any other parameters in each procedure.

VI. Conclusions

In this paper, a new approach for tuning of a vector controller prior to starting of an unknown motor has been developed and demonstrated. The basis of the tuning procedure for determining motor parameters lies in the transient response of the speed and current controller output signal. Observing the shape of the controller output signal of the drive system, the state of detuning is clearly noticeable. Each procedure has a high sensitivity to detuning and is inherently independent of the information of other parameters. All the tuning algorithms have been implemented on an actual inverter system to confirm its feasibility.

References

[1] P. Vas, *Vector Control of AC Machines*. London, U.K.: Oxford Univ. Press, 1990, pp. 122–215.

[2] R. Krishnan and F. C. Doran, "A study of parameter sensitivity in high performance inverter fed induction motor drive system," *IEEE Trans. Ind. Applicat.*, vol. IA-23, pp. 623–635, July/Aug. 1987.

[3] P. Vas, *Parameter Estimation, Condition Monitoring, and Diagnosis of Electrical Machines*. London, U.K.: Clarendon, 1993.

[4] C. Wang, D. W. Novotny, and T. A. Lipo, "An automated rotor time constant measurement system for indirect field oriented drives," *IEEE Trans. Ind. Applicat.*, vol. IA-21, pp. 624–632, May/June 1985.

[5] A. Khambadkone and J. Holtz, "A vector controlled induction motor drive with a self-commissioning scheme," *IEEE Trans. Ind. Electron.*, vol. 38, pp. 322–327, Oct. 1991.
[6] R. D. Lorenz, "A tuning of field-oriented induction motor controllers for high performance applications," *IEEE Trans. Ind. Applicat.*, vol. IA-22, pp. 293–297, Mar./Apr. 1986.
[7] J. R. Willis, G. J. Brock, and J. S. Edmonds, "A derivation of induction motor models from standstill frequency response tests," *IEEE Trans. Energy Conversion*, vol. 4, pp. 608–613, Dec. 1989.
[8] A. Stankovic, E. R. Benedict, V. John, and T. A. Lipo, "A novel method for measuring induction machine magnetizing inductance," in *Conf. Rec. IEEE-IAS Annu. Meeting*, 1997, pp. 234–238.
[9] S. I. Moon and A. Keyhani, "A estimation of induction machine parameters from standstill time-domain data," *IEEE Trans. Ind. Applicat.*, vol. 30, pp. 1609–1615, Nov./Dec. 1994.
[10] H. B. Karayaka, M. N. Marwali, and A. Keyhani, "A induction machine parameter tracking from test data via PWM inverters," in *Conf. Rec. IEEE-IAS Annu. Meeting*, 1997, pp. 227–233.
[11] J. K. Seok, S. I. Moon, and S. K. Sul, "A induction machine parameter identification using PWM inverter at standstill," *IEEE Trans. Energy Conversion*, vol. 12, pp. 127–132, June 1997.
[12] G. F. Franklin, J. D. Powell, and A. Emami-Naeini, *Feedback Control of Dynamic Systems*. Reading, MA: Addison-Wesley, 1988, pp. 15–75.
[13] T. M. Rowan and R. J. Kerkman, "A new synchronous current regulator and analysis of current regulated PWM inverters," *IEEE Trans. Ind. Applicat.*, vol. IA-22, pp. 597–602, Mar./Apr. 1987.
[14] R. Ueda, T. Sonoda, K. Koga, and M. Ichikawa, "A stability analysis in induction motor driven by V/f controlled general purpose inverter," *IEEE Trans. Ind. Applicat.*, vol. 28, pp. 472–481, Mar./Apr. 1992.

Jul-ki Seok (S'94–M'98) was born in Korea in 1969. He received the B.S., M.S., and Ph.D. degrees in electrical engineering from Seoul National University, Seoul, Korea, in 1992, 1994, and 1998, respectively.

He is with the Production Engineering Center, Samsung Electronics Company Ltd., Suwon City, Korea. His specific research interests are electrical machines, high-performance electrical machine drives, and high-power ac drives. Currently, he works on servo drive systems and electromagnetic compatibility of multi-axes drives.

Seung-Ki Sul (S'78–M'87–SM'98–F'00) was born in Korea in 1958. He received the B.S., M.S., and Ph.D. degrees in electrical engineering from Seoul National University, Seoul, Korea, in 1980, 1983, and 1986, respectively.

From 1986 to 1988, he was with the Department of Electrical and Computer Engineering, University of Wisconsin, Madison, as an Associate Researcher . He was a Principal Research Engineer with Gold-Star Industrial Systems Company from 1988 to 1990. Since 1991, he has been with the School of Electrical Engineering, Seoul National University, where he is currently an Associate Professor. His current research interests are power electronic control of electric machines, electric vehicle drives, and power converter circuits.